

Fluorescence of Pyrenyl and Carbazolyl Derivatives in Liquid Solution and Solid Film

Brooke M. Conger, Dimitris Katsis, John C. Mastrangelo, and Shaw H. Chen*

Materials Science Program, Chemical Engineering Department, NSF Center for Photoinduced Charge Transfer and Laboratory for Laser Energetics, Center for Optoelectronics and Imaging, University of Rochester, 240 East River Road, Rochester, New York 14623-1212

Received: July 15, 1998; In Final Form: September 16, 1998

A systematic investigation of the effects of stereochemistry and solid-state morphology on emission characteristics were performed using glass-forming pyrenyl and carbazolyl derivatives as neat films in PMMA and cholesteric liquid crystalline glass. At high dilution in tetrahydrofuran, pyrenyl derivatives were prone to form intramolecular excimers whereas carbazolyl derivatives showed no evidence for excimers. Both pyrenyl and carbazolyl derivatives at 10^{-3} to 10^{-2} M in isotropic and ordered solid hosts exhibited mostly monomer emission. In neat films, intermolecular excimers prevailed in pyrenyl derivatives whereas carbazolyl derivatives showed evidence for monomer emission as well. One feature that distinguishes carbazolyl derivatives from poly(*N*-vinylcarbazole) is the observed fine structures in the fluorescence spectra of thin films. Order parameters characterizing the helical alignment of pyrenyl and carbazolyl pendants with a cholesteric host were determined with circularly polarized fluorescence spectroscopy. The results indicate the relative ease of aligning pyrenyl groups, presumably because of the more favorable regiochemistry and conformational flexibility.

I. Introduction

Organic materials have been extensively explored for optical and electronic applications in view of the inherent versatility through molecular design and synthesis. There are two distinct approaches to materials that are capable of vitrification into thin films, polymeric and low-molar mass in molecular structure. Empirically, low-molar-mass materials are desirable from a processing standpoint because of the relatively low melt viscosity and the potential for vapor deposition into thin films. Although numerous low-molar-mass organic glasses have been reported,^{1–5} it remains a challenging task to design functional materials capable of forming morphologically stable, glassy films with no residual crystallinity that tends to cause optical loss and hinder charge transport at grain boundaries. The term “morphological stability” describes the resistance of a glass or melt to thermally activated recrystallization. As part of our systematic approach to the design of glass-forming organic materials, we have reported amorphous systems consisting of cyclohexane, bicyclo[2.2.2.]oct-7-ene, and adamantane to which pyrenyl and carbazolyl groups are chemically bonded.⁶ Fluorescence spectra in dilute solution were collected to probe the interaction between pendant groups as affected by stereochemistry.

The present study was motivated to illuminate how pendant groups orient themselves in vitrified isotropic and helically aligned films via a systematic investigation of fluorescence in solid films. Furthermore, the relative ease of helically aligning pyrenyl and carbazolyl groups attached to various central cores was quantified in terms of the orientation order parameter, *S*, based on circularly polarized fluorescence (CPF). The analysis of CPF spectra was performed on the basis that the absorption and emission transition moments of monomeric pyrene lie parallel to the long molecular axis⁷ and those of monomeric

carbazole lie along the short molecular axis.⁸ From a practical perspective, blending pyrenyl and carbazolyl derivatives with isotropic and liquid crystalline materials provides an effective means to tailoring film morphology (i.e., order vs disorder) and tuning absorption and emission properties while maintaining glass- and film-forming abilities.

II. Experimental Section

Materials. Figure 1 summarizes the chemical structures of all the materials used in this study. The synthesis and characterization of the glass-forming materials **I–V** have been reported previously.⁶ The hosts used were poly(methyl methacrylate) ($\bar{M}_n = 75\,000$, Polysciences) and **VII**, a cholesteric liquid crystalline siloxane with an average molecular weight of 1900 g/mol as received from Consortium für Elektrochemische Industrie GMBH in Germany. Compound **VI** was synthesized using 3-(*N*-carbazolyl)propanol and 1,3,5,7-tetrakis(chlorocarbonyl)cubane following the procedures described previously.⁶ NMR (QE-300, GE; CDCl₃) spectral data: δ 8.18–7.20 (m, 32H, aromatic), 4.80 (s, 4H, cubane **H**), 4.40 (t, 8H, CH₂CH₂N), 4.18 (t, 8H, COOCH₂CH₂CH₂), 2.27 (p, 8H, COOCH₂–CH₂–CH₂). Anal. Calcd for C₇₂H₆₀N₄O₈: C, 77.96; H, 5.45; N, 5.05. Found: C, 77.58; H, 5.46; N, 4.95.

Thermotropic Properties. Thermal transitions were characterized by a differential scanning calorimeter (DSC, Perkin-Elmer DSC-7) with a continuous nitrogen purge at 20 mL/min. All the samples were preheated to 200 °C followed by cooling at –20 °C/min to –20 °C. The reported phase-transition temperatures were identified from the second heating scans at 20 °C/min. Cholesteric mesomorphism was identified as oily streaks with a polarizing optical microscope (Leitz Orthoplan-Pol) equipped with a hot stage (FP82, Mettler) and a central processor (FP80, Mettler).

Film Preparation and Characterization. Doping of PMMA and **VII** with 1-pyrenemethanol, PM, and **I–IV** was ac-

* To whom all correspondence should be addressed.

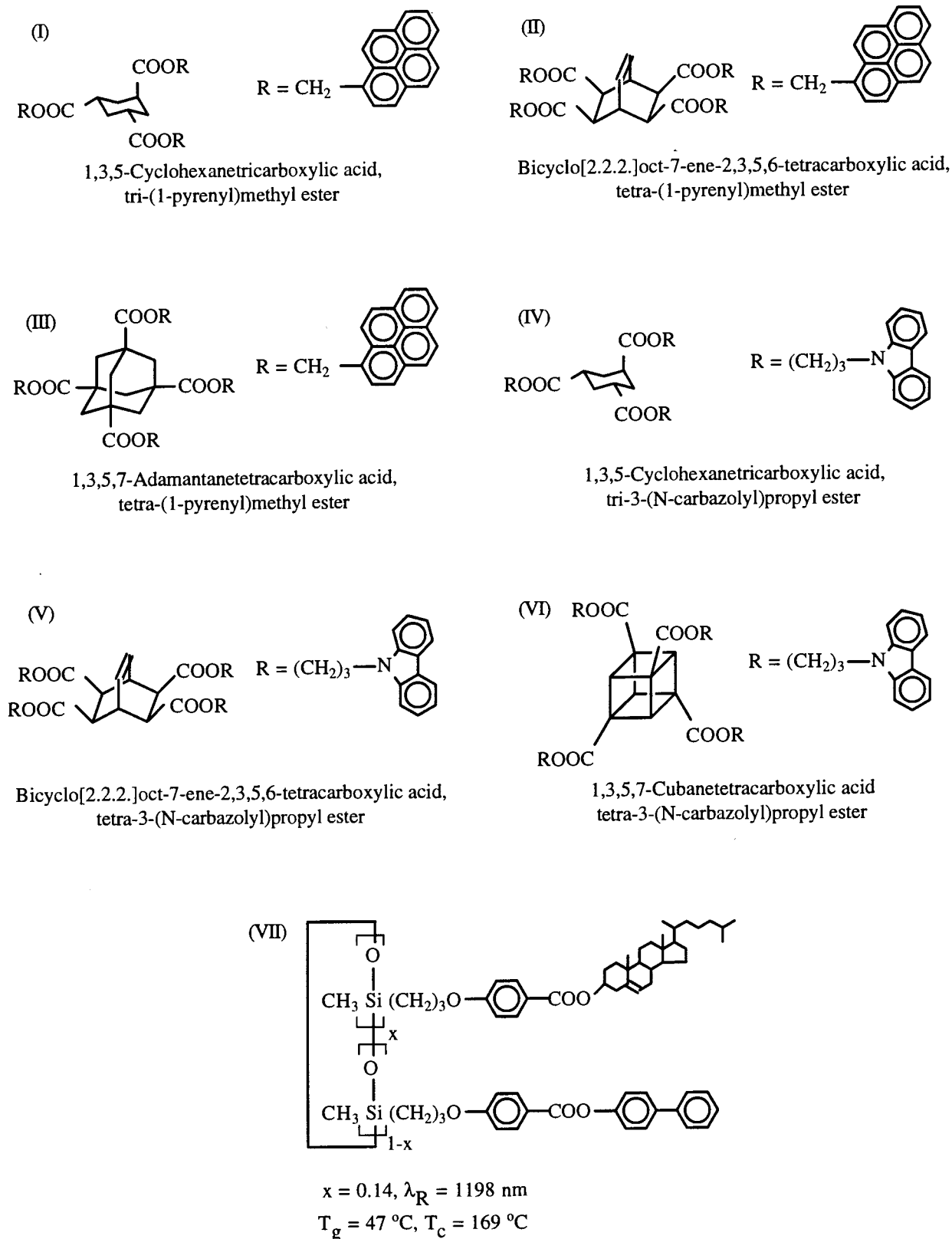


Figure 1. Molecular structures of pyrenyl and carbazolyl derivatives as guests and a cholesteric cyclosiloxane as the host used in this study.

complicated by dissolving the pure components in methylene chloride followed by drying in vacuo. Films of compounds **I–III** in pure form and **VII** lightly doped with **I–IV** were prepared between two fused silica substrates (Escoproducts, 1 in. diameter \times $1/8$ in. thick, with $n = 1.458$), which were coated with Nylon 66 as an alignment layer. The film thickness was controlled at 4 and 18 μm using glass fiber spacers. The

cholesteric devices were heated to 95% of the clearing temperature, T_c , sheared to induce alignment, annealed for 3 h, and subsequently cooled at a rate of 30 $^\circ\text{C}/\text{h}$ to room temperature. Because of the high melt viscosity of PMMA, lightly doped PMMA was prepared by dip coating from methylene chloride solutions, producing single-substrate films. Neat films of carbazole-containing compounds were prepared via spin coating

TABLE 1: Thermal and Optical Properties of Compounds I–VI as Neat Films and Doped into VII and PMMA

compound	host	conc (M) ^a	transition temp (°C)	thickness of film (μm)	g _c	
					RHCP excitation	LHCP excitation
PM	N/A	N/A	K 126 I	N/A		
	PMMA	0.0022	G 113 I	20		
	VII ^b	0.0022	G 48 Ch 170 I	18	−0.12	−0.08
I	neat film	3.5	G 86 I	4		
	PMMA	0.035	G 112 I	27		
	VII ^b	0.035	G 47 Ch 167 I	18	−0.14	−0.11
II	neat film	3.5	G 132 I	4		
	PMMA	0.035	G 112 I	23		
	VII	0.035	G 46 Ch 163 I	18	−0.13	−0.08
III	neat film	3.4	G 119 I	4		
	PMMA	0.034	G 112 I	21		
	VII ^b	0.034	G 47 Ch 164 I	18	−0.14	−0.11
IV	neat film	3.6	G 49 I	0.013		
	PMMA	0.1	G 106 I	1.20		
	VII ^c	0.036	G 45 Ch 160 I	18	0.04	0.04
V	neat film	3.6	G 72 I	0.015		
VI	neat film	3.6	G 67 I	0.040		

^a Concentration expressed in mol/L of pyrenyl or carbazolyl groups with a solid density approximated as 1 g/mL. ^b Excitation at 350 nm; g_c evaluated at 399 nm for I–III and at 391 nm for PM. ^c Excitation at 345 nm; g_c evaluated at 368 nm. ^d Thermal transition temperatures determined from the second heating scans of samples preheated to 200 °C followed by cooling at −20 °C/min to −20 °C; cholesteric mesophase identified as oily streaks under polarizing optical microscope.

from dilute solutions in methylene chloride onto single substrates. The film thickness was limited to 10–40 nm, so that absorption and emission could be accurately measured.

Absorption and Selective Reflection Spectra. A spectrophotometer (Perkin-Elmer Lambda 9) was used to collect the UV–Vis–NIR absorption spectra of isotropic and cholesteric films. The same instrument was used to obtain the selective reflection spectrum of a cholesteric film, and the selective reflection wavelength, λ_R , was determined as the center wavelength of the selective reflection band, which also furnished the average index of refraction, \bar{n} , and optical birefringence, Δn , of quasinematic layers comprising a cholesteric film. In addition, the interference fringes of the air gap sandwiched between the two substrates were measured on the spectrophotometer to calculate the film thickness. The thickness of a single-substrate film was measured on a white light interferometer (Zygo New View 100).

Fluorescence and Excitation Spectra and Decay Dynamics. Steady-state fluorescence, including CPF, measurements were made on a spectrofluorimeter (Perkin-Elmer MPF-66) using the optical setup for polarization control and analysis described previously.⁹ For pyrene derivatives, the excitation wavelength for fluorescence measurements was 350 nm for all films. For carbazole derivatives, the excitation wavelength was 300 nm for neat and PMMA films and 345 nm for doped cholesteric films to avoid absorption by the host. Excitation spectra were measured on a Spex Fluorolog 2 spectrofluorimeter. Fluorescence decays were recorded via time-correlated single-photon counting (SPC) as described previously.⁹

III. Results and Discussion

Thermal and optical properties of 1-pyrenemethanol (PM) and compounds I–III as neat films and lightly doped into PMMA and VII are summarized in Table 1. As a general observation, pyrenyl groups can be chemically integrated into glass-forming materials via functionalization of alicyclic cores with an elevated T_g characteristic of the hybrid structure. Emission from aggregated pyrenyl groups in the ground state, both in THF and in solid films, was ruled out by the overlap of the excitation spectra monitored at the emission maxima with

the absorption spectrum of PM in THF at 10^{-6} M. The fluorescence spectra of pyrenyl derivatives are compiled in Figure 2 to display the effect of the molecular structure of the guest and the microenvironment provided by the host on emission characteristics. In THF at 10^{-6} M, PM shows monomer emission peaks at 380 and 400 nm,¹⁰ I and II show predominantly excimer emission as a broad peak centered at 480 nm,¹⁰ while III shows a balance between the monomer and excimer emission. The excimer formation observed in I and II at high dilution suggests its *intramolecular* origin. On the other hand, it appears that adamantane as the central core for III suppresses excimer formation, presumably because of the stereochemical constraint imposed on the pyrenyl pendants. With solid film densities approximated as 1 g/mL, the doping levels of PM, I, II, and III in PMMA and VII and the concentration of I–III as neat films were calculated in terms of molarity in pyrenyl groups, M. The doping level of PM in PMMA and VII was limited to an order of magnitude less than that for I–III because of the phase separation problem identified under a polarizing optical microscope. The emission spectra in isotropic PMMA and VII at 10^{-3} to 10^{-2} M reveal the absence of excimer formation. Thus, excimer formation is prevented in solid films because of the lack of mobility on the part of pyrenyl pendants. However, fluorescence from neat films produced nothing but excimer emission, as shown for both I and III. The fact that excimers are absent in PMMA and VII films and that they are predominant in neat films indicates the *intermolecular* origin of excimer formation in neat films in which pyrenyl groups apparently are well packed without causing crystallization.

Compound VII is capable of forming a glassy cholesteric film with $T_g = 47$ °C, $T_c = 169$ °C, and $\lambda_R = 1198$ nm. With naturally occurring (−)-cholesterol as the chiral building block, a left-handed (LH) helical structure emerged from a well-aligned film of VII.¹¹ Thus, this cholesteric host is capable of twisting a rodlike guest into a LH helical arrangement at the molecular level, giving rise to CPF. As illustrated in Figure 3a, I at a doping level of 0.035 M in VII presents a selective reflection peak centered at 1190 nm, indicating a negligible disruption to the helical structure of the host. The observed optical density of 0.28 is close to the theoretical limit of 0.30 expected of a

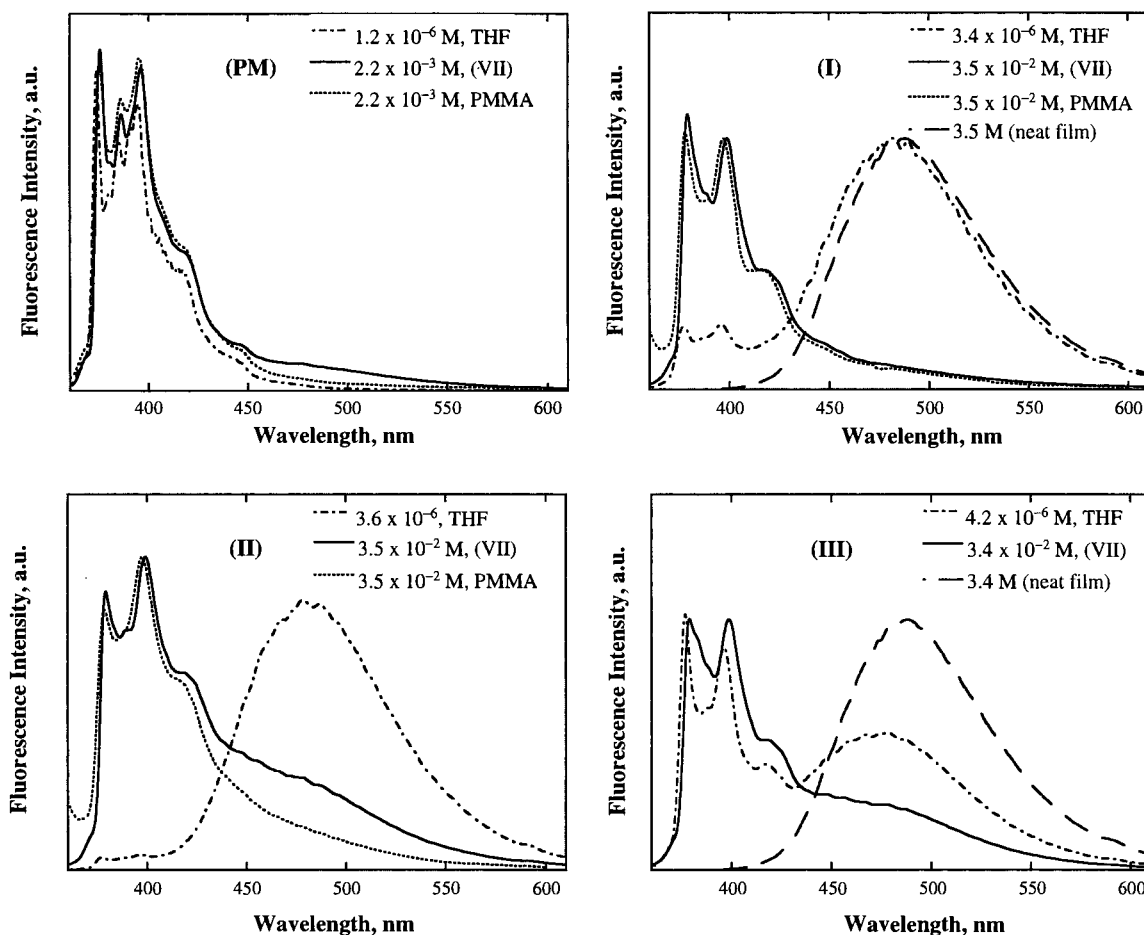


Figure 2. Fluorescence spectra with excitation at 350 nm of pyrenyl derivatives in THF and PMMA and as neat films.

perfectly aligned, single-handed cholesteric film. With both left- and right-handed circularly polarized (LH- and RH-CP) excitations at 350 nm, the CPF spectra are presented in Figure 3b; note the absence of emission from excimers. The degree of CPF was calculated for the emission peak of pyrenyl pendants at 399 nm in terms of $g_e = 2(I_L - I_R)/(I_L + I_R)$, in which I_L and I_R are LH and RH circularly polarized emission intensity, respectively. As a validation of the experimental technique, $g_e = 0.006 \pm 0.005$ was found for the lightly doped, isotropic PMMA films. The calculated g_e values, with an uncertainty of $\pm 5\%$ in general, for all helically aligned films are presented in Table 1. Note that all three pyrenyl derivatives in **VII** showed an emission peak at 399 nm except PM, which was found to undergo a blue shift to 391 nm (see also Figure 2). The negative g_e in a LH host resulted from an emission transition moment lying parallel to the long molecular axis of pyrene.⁷ According to a recent theory,¹² g_e is a function of the average absorption coefficient (i.e., absorbance per unit film thickness), A , at the excitation wavelength, average index of refraction, \bar{n} , and optical birefringence, Δn , both at the emission wavelength. The parameter A was readily determined using doped PMMA films with UV-Vis spectrophotometry. A cholesteric film with a $\lambda_R = 450$ nm, i.e., with $x = 0.14$ in the general structure **VII**, was prepared to afford a selective reflection spectrum. This experimental result was fitted to Good and Karali's theory¹³ to arrive at $\bar{n} = 1.56$ and $\Delta n = 0.11$. As a simplification for data analysis, it was assumed that anisotropic absorption and emission are characterized by a single S . The experimentally measured g_e values were employed for data analysis using the CPF theory, as accomplished previously.⁹ All the input information and the resultant S are summarized in Table 2. Despite the low aspect

ratio of the pyrene molecule and the disparity in molecular structure between **PM**, **I**, **II**, and **III**, the resultant S values characterizing the orientation order of pyrenyl groups are reasonably close to each other.

With excitation at 294 nm, compounds **IV–VI**, 3-(*N*-carbazolyl)propanol, and *N*-ethyl carbazole in methylene chloride at 10^{-6} to 10^{-4} M showed structured fluorescence spectra with peaks at 353 and 368 nm that were attributed to monomer emission.⁶ A single-exponential function was found to represent the SPC data collected at 350, 368, and 440 nm, resulting in a fluorescence lifetime of 6.3 ± 0.3 ns ($1.02 \leq \chi^2 \leq 1.50$) for all these compounds in methylene chloride at 10^{-5} M. A 1.20 μ m thick film of **IV** in PMMA at 0.1 M was also characterized by monomer emission, as evidenced by its normalized fluorescence spectrum overlapping with that of *N*-ethyl carbazole in methylene chloride at 10^{-6} M. To assess the extent to which carbazolyl groups can be aligned in a structured film, **IV** was doped into **VII** at 0.036 M (on the basis of carbazolyl group). With RH- and LH-CP excitations at 345 nm, the CPF spectra bore a close resemblance to monomer emission. The decay dynamics (probed at 368, 393, and 430 nm) was well represented by a single-exponential function with a lifetime of 6.7 ± 0.4 ns ($\chi^2 = 1.32, 1.13, 1.29$). On the basis of the measured CPF intensities at 368 nm, $g_e = 0.04$ was determined. The positive g_e value in a LH host indicates that the emission transition moment lies along the short molecular axis of carbazole, consistent with previous observations.⁸ The best fit to the CPF theory using input information listed in Table 2 led to $S = 0.12$, indicating a relatively poor orientation order assumed by carbazolyl groups in **IV**. Compared to $S = 0.46$ for **I/VII**, carbazolyl groups are more difficult to align in a structured film

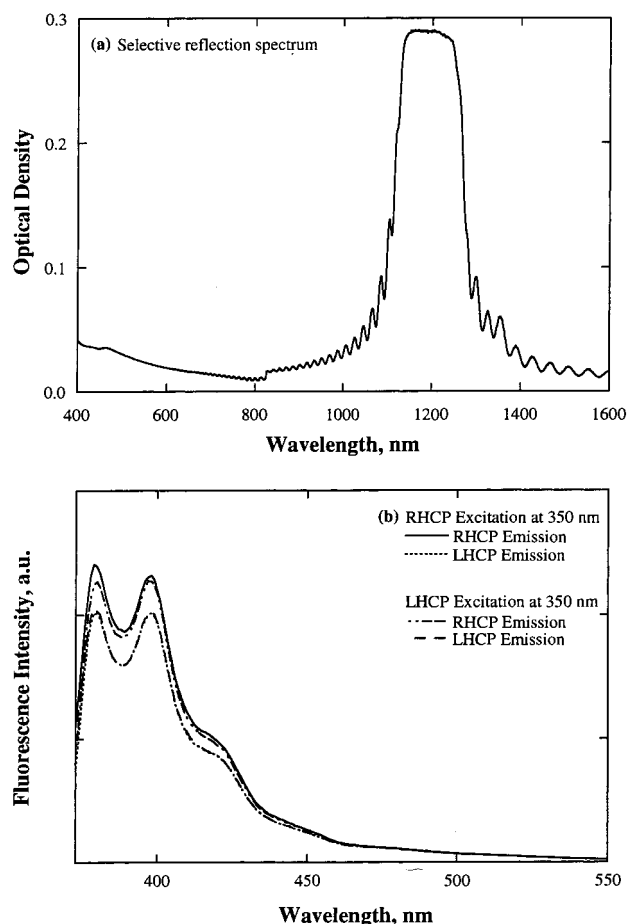


Figure 3. An 18 μm thick solid film of **I** in **VII** at 0.035 M: (a) Selective reflection spectrum; (b) Circularly polarized fluorescence spectra with excitation at 350 nm.

TABLE 2: Input Data and Resultant Orientational Order Parameters for PM and I–IV Doped in VII, a Chiral-Nematic Host

compound	λ_R (nm) ^a	A (cm ⁻¹) ^b	S^c
PM	1197	12	0.37
I	1190	112	0.51
II	1203	143	0.41
III	1182	132	0.52
IV	1195	1345	0.12

^a The center of the selective reflection spectra were identified as λ_R .

^b Isotropic PMMA films were used to measure A at 350 nm for PM and **I**–**III** and at 345 nm for **IV**. ^c Parameter estimation via the best fit for the experimentally measured g_e to a CPF theory¹² with $\Delta n = 0.11$ and $\bar{n} = 1.56$, which were estimated with the selective reflection spectrum of a cholesteric film having $\lambda_R = 450$ nm.

than pyrenyl groups under otherwise identical conditions. The observed difference in ease of alignment may have arisen from the more favorable regiochemistry and conformational flexibility of **I** in comparison to **IV**, consistent with the steady-state fluorescence spectra gathered for both in methylene chloride at high dilution.⁶

To elucidate the role played by stereochemistry in fluorescence from neat solid films, compounds **IV**–**VI** were spin-coated from solution onto fused silica substrates, forming isotropic films with a thickness on the order of tens of nanometers. The absorption spectra of these three films are identical with those of *N*-isopropyl carbazole at 10^{-5} M,¹⁴ thus ruling out the possibility of ground-state association. Furthermore, the excitation spectra of these films mesh well with the

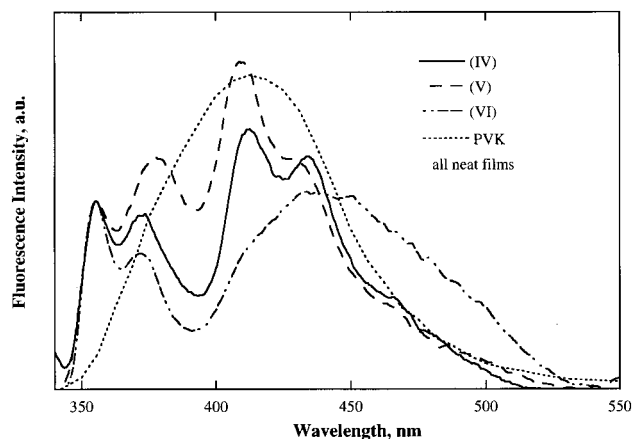


Figure 4. Fluorescence spectra with excitation at 300 nm of carbazolyl derivatives as neat films; fluorescence spectrum of poly(*N*-vinylcarbazole) reproduced from ref 15.

absorption spectra, indicating that monomeric carbazole was the only excitable species. As shown in Figure 4, fluorescence spectra of these neat films are better structured than the single broad peak reported for a solid poly(*N*-vinylcarbazole), PVK, film.¹⁵ Although the peak at 355 nm is attributable to fluorescence of monomeric carbazole, all other peaks at longer wavelengths are contributed by other excited-state species including excimers.¹⁶ Three exponential functions were needed to represent the decay dynamics probed by SPC across the spectral range from 350 to 450 nm. For example, three time constants were found for **IV**: 0.3–0.7, 1–2, and 4–7 ns ($1.00 \leq \chi^2 \leq 1.40$), which differ from previously reported values for various carbazole-containing compounds in solid film¹⁶ or dilute liquid solution.¹⁷ However, one study of PVK in dilute methylene chloride solution did report three lifetimes, 0.11, 1.7, and 15.5 ns,¹⁸ which are largely consistent with the present observation. It appears that the lifetimes resulting from fitting the SPC data to a multitude of exponential functions cannot be readily identified with excited-state species.

IV. Summary

Isotropic solid films were prepared with fluorescent glass-forming pyrenyl and carbazolyl derivatives with T_g ranging from 49 to 132 °C. To investigate the role played by morphology in emission characteristics, these fluorescent compounds were mixed with PMMA and cholesteric cyclosiloxane glass for the preparation of isotropic and helically oriented films. With PM serving as the basis for identifying the sources of emission, **I** and **II** at 10^{-6} to 10^{-5} M in tetrahydrofuran were found to be predominated by *intramolecular* excimers with **III** showing a much reduced tendency. On the other hand, PMMA and **VII** as solid hosts containing pyrenyl derivatives at 10^{-3} to 10^{-2} M exhibited predominantly monomer emission. *Intermolecular* excimers were found to prevail in neat films of **I**–**III**. The helical orientation of pyrenyl groups in PM and **I**–**III** enforced by **VII** permitted the degree of alignment to be quantified by CPF spectroscopy with S values ranging from 0.37 to 0.52, suggesting a minor influence by the central core on the ease of aligning pyrenyl pendants. In contrast to pyrenyl groups, carbazolyl pendants to **IV**–**VI** in methylene chloride at 10^{-6} to 10^{-4} M showed no evidence of excimer formation, as was the case with solid films of PMMA and **VII** containing **IV** at 0.1 and 0.036 M, respectively. It appears that carbazolyl groups are less prone to excimer formation than pyrenyl groups with the same stereochemistry imposed by the central core. The

fluorescence spectra of neat solid films of **IV**–**VI** revealed fine structures in the 350–500 nm spectral range, unlike the structureless spectrum of the PVK film. In comparison to pyrenyl groups in **I**, carbazolyl groups in **IV** are less amenable to helical alignment in **VII** as reflected by an orientational order parameter of 0.12 in comparison to 0.51.

Acknowledgment. The authors express their gratitude for helpful discussions with and technical assistance of Drs. S. D. Jacobs and A. W. Schmid and Mr. K. L. Marshall of the Laboratory for Laser Energetics. This work was supported by the National Science Foundation under Grant Nos. CTS-9500737, CHE-9120001, and CTS-9811172. Additional support was provided by the U.S. Department of Energy Office of Inertial Confinement Fusion under Cooperative Agreement No. DE-FC03-92SF19460, the University of Rochester, and the New York State Energy Research and Development Authority. The support of DOE does not constitute an endorsement by DOE of the views expressed in this article.

References and Notes

- (1) Naito, K.; Miura, A. *J. Phys. Chem.* **1993**, *97*, 6240.
- (2) Lundquist, P. M.; Wortmann, R.; Geletneky, C.; Twieg, R. J.; Jurich, M.; Lee, V. Y.; Moylan, C. R.; Burland, D. M. *Science* **1996**, *274*, 1182.
- (3) Katsuma, K.; Shirota, Y. *Adv. Mater.* **1998**, *10*, 223.
- (4) Zhang, Y.; Wada, T.; Wang, L.; Sasabe, H. *Chem. Mater.* **1997**, *9*, 2798.
- (5) Alig, I.; Braun, D.; Langendorf, R.; Wirth, H. O.; Voigt, M.; Wendorff, J. H. *J. Mater. Chem.* **1998**, *8*, 847.
- (6) Mastrangelo, J. C.; Conger, B. M.; Chen, S. H. *Chem. Mater.* **1997**, *9*, 227.
- (7) (a) Sackmann, E.; Rehm, D. *Chem. Phys. Lett.* **1970**, *4*, 537. (b) Sackmann, E.; Voss, J. *Chem. Phys. Lett.* **1972**, *14*, 528.
- (8) (a) Saeva, F. D. *J. Am. Chem. Soc.* **1972**, *94*, 5135. (b) Kawaguchi, K.; Sisido, M.; Imanashi, Y. *J. Phys. Chem.* **1988**, *92*, 4806.
- (9) Conger, B. M.; Mastrangelo, J. C.; Chen, S. H. *Macromolecules* **1997**, *30*, 4049.
- (10) Förster, Th. *Angew. Chem.* **1969**, *81*, 364.
- (11) (a) Tsai, M. L.; Chen, S. H.; Jacobs, S. D. *Appl. Phys. Lett.* **1989**, *54*, 2395. (b) Tsai, M. L.; Chen, S. H. *Macromolecules* **1990**, *23*, 1908.
- (12) Shi, H.; Conger, B. M.; Katsis, D.; Chen, S. H. *Liq. Cryst.* **1998**, *24*, 163.
- (13) Good, R. H., Jr.; Karali, A. *J. Opt. Soc. Am. A* **1994**, *11*, 2145.
- (14) Pearson, J. M.; Stolka, M. *Poly(vinylcarbazole)*; Polymer Monographs; Gordon and Breach Science Publishers: New York, 1981; Vol. 6, Chapter 8.
- (15) Masuhara, H.; Tamai, N.; Ikeda, N.; Mataga, N.; Itaya, A.; Okamoto, K.; Kusabayashi, S. *Chem. Phys. Lett.* **1982**, *91*, 113.
- (16) Itaya, A.; Okamoto, K.; Kusabayashi, S. *Bull. Chem. Soc. Jpn.* **1977**, *50*, 22.
- (17) (a) Kitamura, N.; Inoue, T.; Tazuke, S. *Chem. Phys. Lett.* **1982**, *89*, 329; (b) Keyanpour-Rad, M.; Ledwith, A.; Johnson, G. E. *Macromolecules* **1980**, *13*, 222.
- (18) Ghiggino, K. P.; Archibald, D. A.; Thistlethwaite, P. J. *J. Polym. Sci., Polym. Lett. Ed.* **1980**, *18*, 673.